JACS
JOURNAL OF THE AMERICAN CHEMICAL SOCIETY
Article
pubs.acs.org/JACS

Rational Design of a Colorimetric pH Sensor from a Soluble Retinoic Acid Chaperone

Tetyana Berbasova, Meisam Nosrati, Chrysoula Vasileiou, Wenjing Wang, Kin Sing Stephen Lee, Ipek Yapici, James H. Geiger,* and Babak Borhan*

Department of Chemistry, Michigan State University, East Lansing, Michigan 48824, United States

Supporting Information

ABSTRACT: Reengineering of cellular retinoic acid binding protein II (CRABPII) to be capable of binding retinal as a protonated Schiff base is described. Through rational alterations of the binding pocket, electrostatic perturbations of the embedded retinylidene chromophore that favor delocalization of the iminium charge lead to exquisite control in the regulation of chromophoric absorption properties, spanning the visible spectrum (474−640 nm). The pK_a of the retinylidene protonated Schiff base was modulated from 2.4 to 8.1, giving rise to a set of proteins of varying colors and pH sensitivities. These proteins were used to demonstrate a concentration-independent, ratiometric pH sensor.

INTRODUCTION

Protein design in general,[1] and design of protein fusion probes with specific spectroscopic properties in particular, has attracted substantial recent interest.[2] For most systems modulation of the color requires the modification of the chromophore itself.[3] More recent studies describe systems that utilize metal ion coordination or quantum dot technology, both of which can potentially disturb cell homeostasis.[4] Another plausible approach is to alter the absorption of a single protein-embedded chromophore through changes in the surrounding protein environment, such that a range of colors could be realized. Nature has demonstrated the potential usefulness of this approach in systems such as the imidazolidinone chromophore in green fluorescent protein (GFP), with emission from cyan to greenish-yellow variants,[5] and the retinylidene-bound rhodopsins required for color vision.[6] Understanding the principles that govern spectroscopic characteristics of protein/chromophore complexes can lead to more specifically designed systems with potential use as tools in molecular and cell biology.

In our recent work, we have focused on the redesign of orthogonal protein systems to recapitulate the wavelength regulation seen in the visual rhodopsin pigments. We initiated this effort by redesigning cellular retinoic acid binding protein II (CRABPII) to bind all-*trans*-retinal as a protonated Schiff base (PSB) (Figure 1a) by introducing an active site Lys residue with the correct trajectory to react with the carbonyl of the bound retinal chromophore.[7] Disappointingly, mutants based on this first-generation system were not capable of modulating the wavelength of the bound retinylidene chromophore. This was ascribed to the buffer-exposed β-ionone ring of the retinal (Figure 1b). The strong polarity of the aqueous media compromised the pigment's ability to respond to electrostatic contributions of nearby amino acids, effectively dampening their influence.[8] This hypothesis was further confirmed by the demonstration of wavelength regulation with a shorter C15-retinal analog, which was fully embedded within the binding site of CRABPII.[8]

In previous work, wavelength regulation of the full-length retinal chromophore was achieved by reengineering a different protein, human cellular retinol binding protein II (hCRBPII). The latter protein binds retinal as a PSB deeper in the binding pocket, as confirmed by crystal structures of several mutants.[9] Interestingly, unlike other reported PSB-forming systems, engineering of a counteranion for the PSB proved unnecessary for this system. A series of hCRBPII mutants led to exceptional regulation of the absorption properties of the bound retinylidene chromophore. From these studies an overall strategy for producing the most bathochromically shifted pigments has emerged: (1) the chromophore must be fully embeded within the binding pocket of the protein; (2) the binding pocket must be isolated as much as possible from the aqueous media; (3) the protonation of the Schiff base must be stabilized in the absence of either a directly interacting counteranion or one that is in the vicinity of the PSB; (4) appropriate amino acids along the length of the polyene must be positioned to project a uniform and relatively neutral electrostatic field, leading to maximal conjugation of the resonating positive charge. These expectations were borne out in dramatic fashion as hCRBPII mutants bound to retinal resulted in absorption maxima that ranged from 425 to 644 nm. This represents a significantly larger wavelength range than that

Received: May 15, 2013
Published: September 20, 2013

   dx.doi.org/10.1021/ja404900k | J. Am. Chem. Soc. 2013, 135, 16111−16119

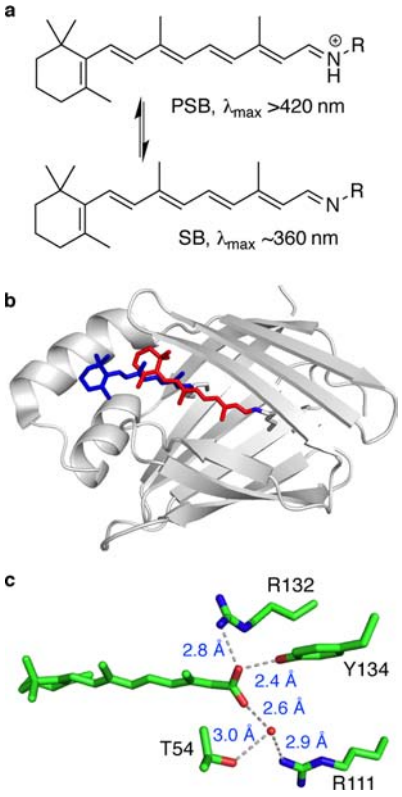

Figure 1. (a) Protonation/deprotonation of the imine triggers a large change in the absorption of the retinylidene chromophore. (b) Overlay of the crystal structure of CRABPII-R132K:R111L:L121E (PDB: 2G7B) with the model structure of CRABPII-R111K, both bound to all-*trans*-retinal (blue and red colored, respectively). The retinal bound through R111K (red) is ~6 Å deeper inside the binding cavity. (c) All-*trans*-retinoic acid bound inside the WT-CRABPII cavity. All the residues identified as important for retinoic acid binding have been highlighted.

of the natural rhodopsins that bind any of the isomeric forms of retinal (420−587 nm).[10]

The titratable iminium proton of the retinylidene PSB provides an ideal mechanism for switching on and off an observable spectroscopic signal (see Figure 1a). The imine (Schiff base, SB) absorbs at ~360 nm, irrespective of the protein environment,[11] while the iminium (protonated Schiff base, PSB) red shifts dramatically with a wavelength maximum that is dependent on the protein sequence.[11,12] Factors that control the acidity of the iminium can effectively lead to a set of protein targets that change color as a function of the pH. The ability to control both the absorption wavelength and the pK_a of the PSB would yield a chromophoric protein-based pH sensor.

Though small organic molecules and nanoparticles are used as both general pH indicators and as intracellular pH sensors,[4,13] issues with specific localization in cellular compartments and potential toxicity with these agents make DNA-encoded protein-based probes superior agents for many pH-sensing applications.[2e,4,14] Most genetically encoded pH probes belong to the GFP family. Among these, ecliptic and ratiometric variants of pHluorins[14c] have found utility in various platforms.[15] The pH sensing ability of pHluorins arises from the titratable protonation state of Tyr66, leading to two excitation maxima. The red ratiometric variant, pHRed, derived from mKeima is another example of a fluorescent pigment with two excitation maxima and a single emission wavelength.[16] pHusion, the fusion product of EGFP and mRFP, has been used as a ratiometric pH sensor for plants.[17] Other pH sensors such as synapto-pHluorin[18] and sypHTomato[14f] were generated from fusion with synaptic vesicle proteins for the imaging of neurotransmitter release.

The proteins reported herein introduce a completely different class of genetically encoded pH probes rationally designed with a minimum amount of mutations from a parent protein with no properties as such at the onset. Even more importantly, they are chromophorically active upon protonation under acidic conditions as opposed to GFP variants, which lose fluorescence at pH below 4.5.[18a,19] From a protein design standpoint, we demonstrate the efficacy of our wavelength modulation strategy by re-engineering our original target, CRABPII, that failed to demonstrate wavelength regulation of bound retinal. The second-generation CRABPII mutants are capable of modulating the absorption of retinylidene PSB over a range of wavelengths similar to that demonstrated for hCRBPII. The potential usefulness of this approach is further demonstrated by the production of a series of protein-based chromophoric pH sensors based on the CRABPII template. These sensors detect pH over a broad range and report in a variety of colors. This proof-of-principle report describes the elements necessary for the design and development of genetically encoded pH probes based on the absorption of retinal. Though the inherently weak fluorescence of retinal has shown some application in vivo,[20] future development will entail the use of highly fluorescent chromophores for further applications.

■ RESULTS AND DISCUSSION

Since the first-generation CRABPII system failed to regulate the wavelength of bound retinylidene absorption, as a result of having a partially solvent-exposed chromophore, the second incarnation entailed the design of a new active site more deeply embedded in the binding cavity. As such, the bound retinal would be completely encapsulated. As described below, this second generation of CRABPII mutants not only succeed in recapitulating the wavelength regulation previously achieved with hCRBPII but also exhibit a wide range of retinylidene pK_a values, making them ideally suited for development of protein-based pH sensors.

Reengineering the Binding Cavity of CRABPII. In silico analysis (see Supporting Information (SI) for details) identified Arg111 as an ideal site to place the PSB-forming Lys residue, given its anticipated trajectory relative to the bound retinal. More significantly, the retinylidene SB would reside about 6 Å deeper in the CRABPII binding cavity as compared to the original R132K:R111L:L121E-CRABPII mutant (Figure 1b). Although the R111K-CRABPII single mutant bound retinal with relatively high affinity (K_d = 460 nM), it did not produce a Schiff base (Table 1, entry 2; Figure S3, SI). From close inspection of the model system we surmised that this could be due to either: (1) the inability of retinal to slip lower into the binding cavity due to interactions with amino acids that stabilize binding in the original location or (2) the presence of hydrophilic amino acids known to interact directly with the carboxylate of retinoic acid (the natural substrate of the wild-type protein), which would not interact favorably with a hydrophobic polyene. Three amino acids (Arg132, Tyr134, and Thr54), known to hydrogen bond with the native substrate, retinoic acid, were targeted for mutagenesis (Figure 1c).

dx.doi.org/10.1021/ja404900k | J. Am. Chem. Soc. 2013, 135, 16111−16119

Table 1. Reengineering of CRABPII and Its Wavelength Regulation

	CRABPII mutants	λ_{max} (nm)[a]	K_d (nM)
1	R132K:R111L:L121E (KLE)[b]	449	1 ± 4.9
2	R111K	385	460 ± 34
3	R111K:R132L	527[c]	63 ± 5
4	R111K:R132L:Y134F	525	54 ± 13
5	R111K:R132L:Y134F:T54V (KLFV)[b]	534	5 ± 9
6	KLFV:L121D	474[d]	2.6 ± 5
7	KLFV:L121N (**M8**)	482	10 ± 7
8	KLFV:L121Q (**M5**)	492	13 ± 12
9	KLFV:L121Q:R59W (**M7**)	513	18 ± 9
10	KLFV:L121Q:R59Y:A32W (**M6**)	538	1.3 ± 2
11	KLFV:R59W	556	162 ± 30
12	KLFV:R59Y	561	111 ± 30
13	KLFV:R59Y:A32Y:A36Y	574	273 ± 29
14	KLFV:R59Y:A32W	591	188 ± 25
15	KLFV:R59W:A32W (**M3**)	610	112 ± 17
16	KLFV:R59W:A32W:E73A (**M13**)	620	71 ± 13
17	KLFV:R59W:A32W:M93L:E73A:S12D	640	38 ± 17

[a]UV−vis spectra of the indicated mutants bound to all-*trans*-retinal at pH 5.0 (citric acid buffer). [b]KLE and KLFV stand for R132K:R111L:L121E and R111K:R132L:Y134F:T54V, respectively. [c]Deconvolution of overlapping peaks was applied. [d]UV−vis spectra were measured at pH 3.0 (citric acid buffer).

Arg132 is a crucial residue for the binding of retinoic acid with CRABPII and in theory could interact with retinal and hinder it from slipping down to the new binding site (Figure 1c). Mutation to Leu (R111K:R132L) resulted in a protein with better affinity for retinal and competent for SB formation (Table 1, entry 3). Schiff base formation was verified by UV−vis and Q-TOF-MS analysis (Figure S4, SI). However, protonation of the SB was difficult even at pH 5. Deconvolution of the UV−vis spectrum measured at pH 5 (Figure S4, SI) uncovered a significantly red-shifted absorption at 527 nm. Since replacement of Arg132 proved to be essential to induce SB formation, the R132L mutation was maintained in the design for most of the mutants. Tyr134 also interacts with retinoic acid in the wild-type protein complex and is relatively close to Arg132 (Figure 1c).[21] The triple mutant R111K:R132L:Y134F (Table 1, entry 4) is not only capable of SB formation at physiological pH but also produces a clear absorption maximum at 525 nm (pH 5.2). Removal of the last polar amino acid, Thr54, results in the tetramutant R111K:R132L:Y134F:T54V. This mutant exhibits further improved binding affinity for retinal and also red shifts 9 nm as compared to its parent triple mutant R111K:R132L:Y134F at pH 5.2 (Table 1, entries 4 and 5).

Overall, the new generation of CRABPII mutants has PSB pK_a values lower than those of the first-generation CRABPII and hCRBPII mutants. This is much better suited for the pH regimes of most physiologically relevant processes. What follows is a description of two sequential goals to ultimately arrive at a series of proteins that are well-suited for pH sensing applications. The first objective is to generate a series of CRABPII mutants capable of regulating the wavelength of absorption through rational design principles. The second goal is to produce a library of chromophoric proteins that change color in response to pH changes in their environment. These mutants will provide a platform for the design of protein-based pH sensors.

Wavelength Regulation Using CRABPII Mutants. The bathochromic shift observed with the second-generation mutants in comparison with the previously engineered R132K:R111L:L121E-CRABPII (Table 1, entry 1) highlights the importance of embedding the chromophore fully within the binding pocket to regulate the wavelength of absorption. Our prior studies highlighted the need to not only embed the chromophore and enclose the binding cavity but also evenly distribute the cationic charge along the polyene for maximal bathochroism.[9] This logic was applied for the wavelength regulation of the second-generation CRABPII mutants.

The R111K:R132L:Y134F:T54V-CRABPII tetramutant (KLFV), exhibiting high retinal affinity and PSB absorption at 534 nm (Table 1, entry 5), was chosen as the parent protein for further mutagenesis to produce blue- and red-shifted pigments. Mutations of L121D, L121N, and L121Q near the iminium nitrogen (Figure 2a) are predicted to localize charge at the PSB and discourage conjugation along the polyene. Indeed, all three mutants blue-shifted the absorption 30−60 nm with L121D contributing the most to the hypsochromic shift (Table 1, entries 6−8).

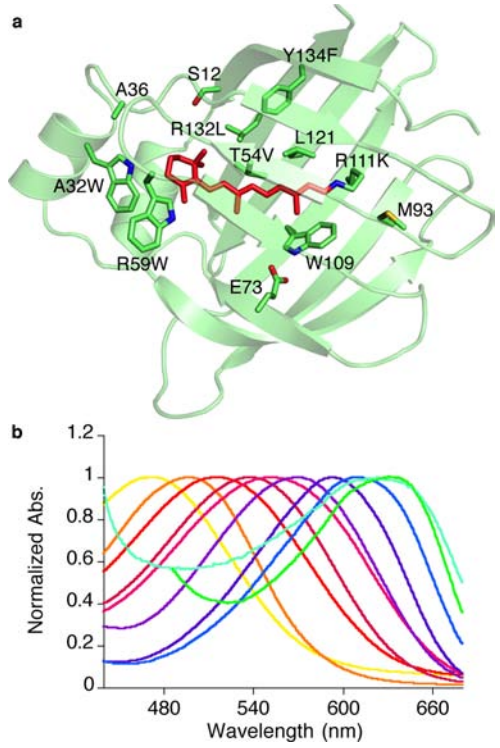

Figure 2. (a) Crystal structure of CRABPII-R111K:R132L:Y134F:T54V:R59W:A32W bound to all-*trans*-retinal (red) as a PSB through Lys111 (PDB: 4I9R). Important amino acids around the retinylidene that were mutated and are discussed in the text are highlighted. (b) Normalized UV−vis spectra of selected CRABPII mutants from Table 1 (acquired at pH = 5), with absorbance maxima ranging between 474 nm (CRABPII-R111K:R132L:Y134F:T54V:L121D) and 640 nm (CRABPII-R111K:R132L:Y134F:T54V:R59W:A32W:M93L:E73A:S12D).

Conversely, to obtain bathochromically shifted pigments, the plan included both removal of the PSB counteranion and the generation of a binding cavity that would lead to an even distribution of electrostatic potential across the length of the polyene. The latter two changes are predicted to lead to maximum conjugation of the positive charge. We began by

dx.doi.org/10.1021/ja404900k | J. Am. Chem. Soc. 2013, 135, 16111−16119

Table 2. pK_a Values of Selected CRABPII Mutants for Design of a pH-Sensing Chromophoric Protein System[a]

	CRABPII mutants	pK_a	color[b]	λ_{max}[c]	λ_{max}[d]	ε[e]
1	R111K:R132Q:Y134F:T54V:R59W:A32W (**M1**)	8.1	blue	618	616	45 600
2	R111K:R132Y:Y134F:T54V:R59W:A32W (**M2**)	7.5	blue	619	619	40 200
3	R111K:R132L:Y134F:T54V:R59W:A32W (**M3**)	7.0	blue	610	610	43 500
4	R111K:R132L:Y134F:T54V:L121Q:R59Y:A32W (**M4**)	5.9	pink	538	538	40 900
5	R111K:R132L:Y134F:T54V:L121Q (**M5**)	5.3	red	492	492	38 600
6	R111K:R132L:Y134F:T54V:L121Y:R59Y:A32W (**M6**)	5.1	pink	529	529	41 400
7	R111K:R132L:Y134F:T54V:L121Q:R59W (**M7**)	4.4	red	505	513	38 800
8	R111K:R132L:Y134F:T54V:L121N (**M8**)	4.2	orange	495	482	47 000
9	R111K:R132L:Y134F:T54V:L121Q:R59W:A32W:M93L:E73A (**M9**)	4.1	purple	560	538	47 200
10	R111K:R132L:Y134F:T54V:L121Y:R59W:A32W:M93L:E73A (**M10**)	3.0	pink	530	530	38 400
11	R111K:R132L:Y134F:T54V:L121Y:R59W (**M11**)	2.8	red	504	504	36 100
12	R111K:R132Q:Y134F:T54V:R59W:A32W:M93L:E73A (**M12**)	2.6	cyan	630	607	38 900
13	R111K:R132L:Y134F:T54V:R59W:A32W:E73A (**M13**)	2.4	cyan	620	606	—[f]

[a]The proteins selected demonstrated time-stable pK_a behavior for a minimum of 12 h. [b]Color of the CRABPII/retinal complex in solution at pH equal to or lower than the pK_a value; at pH 1.5 units higher than the pK_a, all the mutants were pale yellow (361−375 nm, color of SB). [c]The λ_{max} observed at high pH (∼1 unit above pK_a). [d]The λ_{max} observed at low pH (∼1 unit below pK_a). [e]Molar extinction coefficients of the λ_{max} in the CRABPII/retinal complex for the acidified sample. [f]The complex nature of the UV−vis spectrum did not allow for an accurate calculation of ε.

enclosing the binding cavity to isolate the polyene from the bulk medium and thus enhance the effect of amino acid mutations in maximizing the bathochromic shift. To this end, Arg59, located at the mouth of the binding cavity, was changed to a number of different amino acids (Table S2, SI). As expected, the largest red-shifts were observed with large hydrophobic residues (R59W and R59Y), presumably because the large aromatic amino acids better shield the protein cavity from the bulk medium (Table 1, entries 11 and 12).

The crystal structure of the R111K:R132L:Y134F:T54V:R59W/retinal complex confirmed the formation of the retinylidene PSB (Figure S5, SI). Furthermore, as shown in Figure 1b and Figure S5 (SI), the chromophore is located approximately 6 Å deeper inside the protein cavity relative to the first-generation CRABPII (R132K:R111L:L121E-CRABPII). Unfortunately, however, the structure also illustrates that the loop containing amino acids S55−T60 had moved substantially (∼4 Å), creating a more open, solvent-accessible binding cavity (Figure S5, SI). To more completely close this portal, Ala32 and Ala36 were targeted for mutagenesis. In silico modeling of the R111K:R132L:Y134F:T54V:R59Y mutant with A32Y and A36Y predicted effective packing and encapsulation of the bound retinal. Indeed, R111K:R132L:Y134F:T54V:-R59Y:A32Y:A36Y leads to an additional 13 nm bathochromic shift (Table 1, entry 13). However, the most significant red-shift is observed by introducing the even larger Trp residue at position 32. Mutation of Ala32 to Trp in R111K:R132L:Y134F:T54V:R59Y and R111K:R132L:Y134F:T54V:R59W results in a 30 and 54 nm red-shift, respectively (Table 1, entries 14 and 15). The crystal structure of R111K:R132L:Y134F:T54V:R59W:A32W clearly illustrates that both tryptophan residues contribute to isolate the bound chromophore from the bulk medium, leading to the large observed bathochromic shift (Figure S6, SI).

Having embedded the chromophore and enclosed the binding pocket, we then focused on evenly distributing the electrostatic potential along the binding pocket. This was achieved by removing a carboxylate from the PSB region (E73A, ∼7.5 Å away from the polyene) and placing a carboxylate in the ionone ring region (S12D, ∼9 Å away from the β-ionone ring). Together, these mutations led to a 30 nm red-shift, yielding a pigment that absorbed maximally at 640 nm (Table 1, entry 17). The placement of carboxylates far from the resonating polyene was critical since we had previously demonstrated that strong anionic interactions close to the polyene blue-shift absorption, presumably as a result of localizing charge in lieu of conjugation.[9]

Normalized UV−vis spectra of selected mutants from Table 1 are depicted in Figure 2b. The pigments at high pH absorb at 365 nm (indicative of SB formation) and after acidification yield the illustrated absorbance maxima for different mutants. Overall, the wavelength of the retinylidene PSB is modulated over 166 nm. The second-generation CRABPII system illustrates the ability to regulate the wavelength of the bound retinal PSB by *embedding* and *enclosing* the chromophore and evenly *distributing* the cationic charge along the polyene, resulting in hyper-shifted spectra beyond what is possible in a homogeneous medium.[22]

pH-Dependent Properties of CRABPII Mutants. The initial aim of this reengineering effort was to demonstrate the ability to recapitulate wavelength regulation, based on principles we have recently discovered, in a protein system that had failed to regulate the wavelength of a bound retinylidene. The second and more significant aim was to explore the ability to modulate the pK_a of the iminium such that the pigments could function as reporters of acidity. The hCRBPII mutants (the original proteins used to demonstrate wavelength regulation) exhibited pK_a values for the PSB that were outside the useful range for physiological studies. On the other hand, the initial CRABPII mutants had lower pK_a values that were better matched with physiologically relevant pH values. We therefore set out to alter the pK_a of the second-generation CRABPII mutants and generate systems that would respond and change color in the physiologically relevant pH regime.

The idea of altering the pK_a of the retinylidene−protein complex finds its inspiration from nature's ability to drastically alter the pK_a of the iminium in different rhodopsins. These pigments exhibit pK_a values that range from 9 to greater than 16.[23] In comparison, the pK_a of the iminium generated from retinal and *n*-butylamine in methanol/water is 7.2.[24] In part, rhodopsins increase the pK_a by stabilizing the iminium through a properly placed counteranion[23d] or long-range interactions

with a counteranion mediated by water or polar amino acids.[20a,25] Furthermore, in addition to the distance, the orientation of the interacting polar residues that stabilize the iminium is important and leads to the observed increase in the pK_a. For our purpose, we envisioned a protein−iminium system that is already devoid of a stabilizing counteranion. That, in combination with the increased hydrophobicity in the PSB region, leads to a decrease of the retinylidene PSB-pK_a. Surprisingly, our initial results, listed in Table 2, indicated that the conformation of the bound chromophore can also modulate the pK_a of the retinylidene, as will be described below.

The search for suitable pH sensors began with the most stable CRABPII mutants (pigment stability over time, minimum of 12 h at room temperature) that showed a broad range of pK_a values and also exhibited varied colors. The mutants that fit the latter criteria are listed in Table 2. Since the absorption of all retinylidene SBs, irrespective of the protein they are bound to, occurs in the UV (<375 nm), the observed color of the imine is pale yellow in solution. It is only upon protonation of the SB that the pigment gains visible color, which is observed maximally below the pK_a of the iminium.

A casual screen of the data does indicate reasonable correlation between the overall polarity of the binding pocket and the observed changes in the pK_a of the retinylidene. Entries 1−3 (Table 2) exhibit successively lower pK_a values (8.1 → 7.5 → 7.0, respectively), which correlate with the increased hydrophobicity of the mutants (R132Q → R132Y → R132L, respectively). However, there is also a set of mutants that gave a large working range of pK_a values but were difficult to rationalize solely based on changes in polarity of the binding pocket. For example, comparison of entries 3 and 13 reveals that a single mutation (E73A), which lies ∼9 Å away from the iminium nitrogen, leads to a >4 pK_a unit decrease. This is not a singular example; in fact, most comparisons in Table 2 exhibit a change in pK_a that is far greater than that expected solely based on a change in polarity.

The latter observations, namely, the lack of correlation of the retinylidene pK_a of a number of mutants with a physical parameter, remained puzzling until the fortuitous discovery that the mutant R111K:R132L:Y134F:T54V:R59W (Table 1, entry 11) exhibited a time-dependent change in pK_a (Figure 3 and Figure S1, SI). Upon incubation with retinal, the PSB was fully formed within 10 min (λ_{max} = 556 nm), with a measured pK_a of 6.6. However, a time-dependent reduction in the intensity of the PSB was noted for the bound complex, as depicted in Figure 3a. Close examination of the changes in the UV−vis spectra suggested that the PSB (556 nm) was converting to the SB (365 nm) and not free retinal (380 nm) (Figure 3). Within 2 h the conversion was complete, with no apparent PSB present based on UV−vis analysis. Acidification of the mature protein complex did recover the PSB absorption (543 nm), clearly indicating that the protein was not denatured. Although the wavelength had blue-shifted slightly (13 nm), it does indicate that the overall polarity of the binding pocket had not changed greatly. Interestingly, titration of the time-matured protein complex indicates a change in the pK_a of the system from the original 6.6 to 2.5 (Figure 4). This explains the gradual loss of the PSB peak as depicted in Figure 3b since the protein complex was incubated in a citric acid buffer with a pH of 5.2. The change in the pK_a of the retinylidene complex to below the pH of the solution leads to the deprotonation of the PSB, yielding the familiar SB absorption at 365 nm.

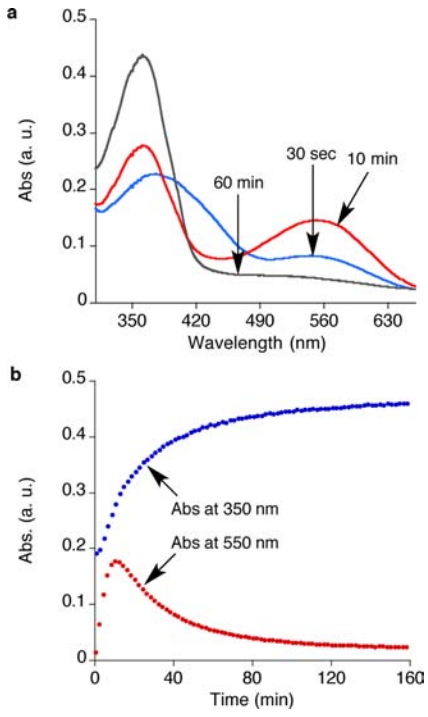

Figure 3. (a) Time-dependent UV−vis spectra of CRABPII-R111K:R132L:Y134F:T54V:R59W bound to all-*trans*-retinal. (b) Time course binding plot of CRABPII-R111K:R132L:Y134F:T54V:R59W with retinal at 25 °C suggests the formation of an initial kinetic complex, exhibiting a higher PSB pK_a, which converts to a thermodynamic complex in 2 h, exhibiting a lower PSB pK_a. Time course analysis over a 2 h period does not indicate any isomerization of the bound all-*trans*-retinal (see SI for details).

The slow change in the PSB of retinal-bound R111K:R132L:Y134F:T54V:R59W CRABPII can only result from changes in the local environment that ultimately lead to stabilization or destabilization of the iminium. Clearly proton exchanges are fast, limited by the rate of diffusion, and thus the observed change in the protonation state must result from a change in the structure of the complex. This is either a result of changes in the structure of the protein, the conformation of the chromophore, or both. What is most likely, since the greatest effect is seen in the pK_a of the iminium, is a change that is closely related to the interaction of the PSB with its protein environment. This could arise from the geometric isomerization of the iminium (*cis* to *trans* or vice versa), presumably from an initially observed kinetic product to a more thermodynamically stable state, that greatly alters the interaction of the iminium nitrogen atom with its surroundings (Figure 4).

A plausible explanation was revealed upon close examination of crystal structures of a few mutants. The data for R111K:R132L:Y134F:T54V:R59W bound to retinal exhibit electron density of sufficient quality to enable assignment of the iminium as *trans*. Since the solution that produced the crystal was incubated for 7 days, we presume the structure of the protein complex to be the one that yields the pK_a of 2.5 (the mature protein). Inspection of the iminium's immediate surroundings reveals a hydrophobic pocket with no discernible interactions with the putative proton of the PSB (Figure 4b, right). The immediate environment of the imine is lined with hydrophobic residues (Ile43, Leu119, and Leu121), thus leading to the low pK_a of the iminium.

dx.doi.org/10.1021/ja404900k | J. Am. Chem. Soc. 2013, 135, 16111−16119

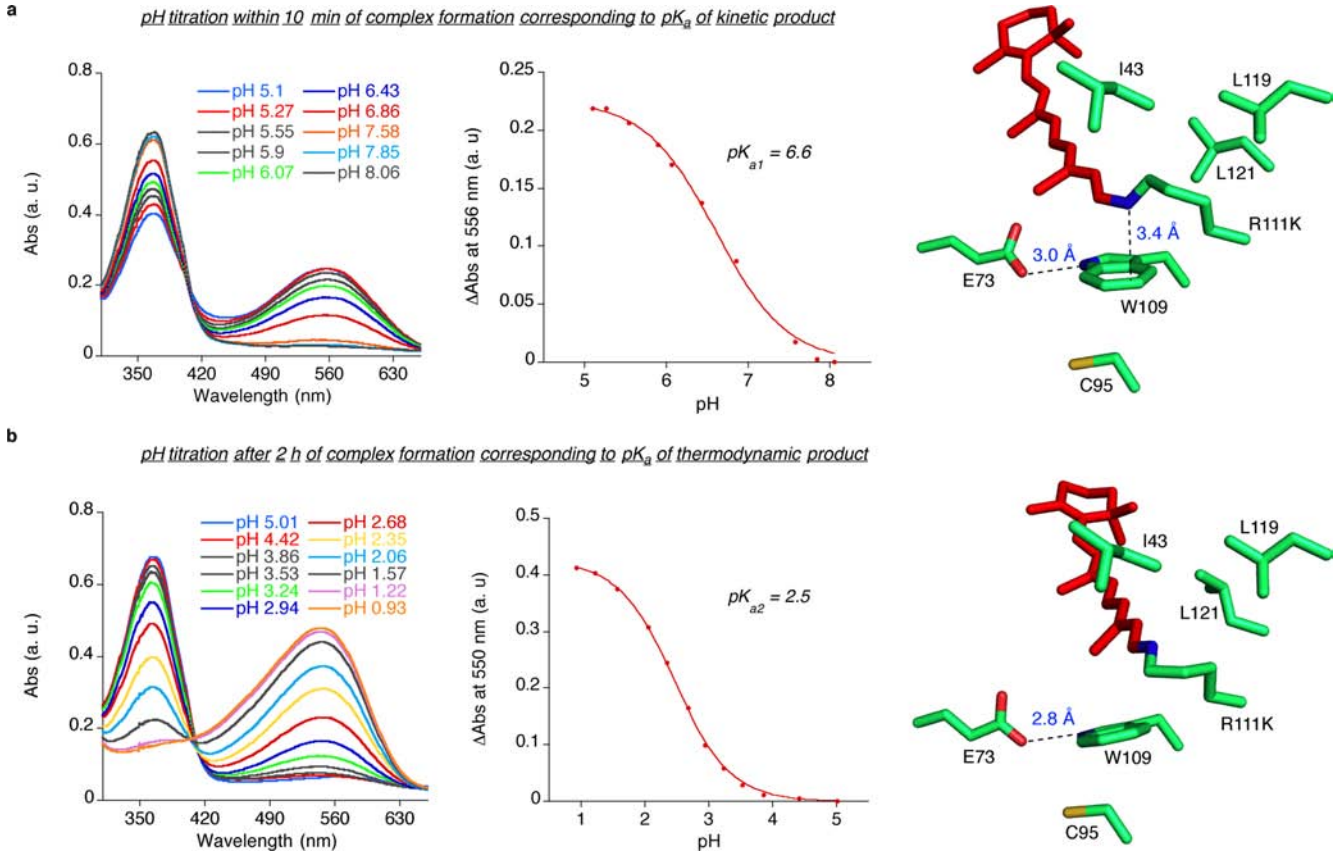

Figure 4. (a) pH titration of the putative kinetic complex (10 min) formed between CRABPII-R111K:R132L:Y134F:T54V:R59W and all-*trans*-retinal (left panel); the PSB pK_a calculated for the kinetic product is 6.6 (middle panel); model structure of the CRABPII-R111K:R132L:Y134F:T54V:R59W mutant (based on the CRABPII-R111K:R132L:Y134F:T54V:R59W crystal structure) with a *cis*-imine geometry (right panel). (b) pH titration of the putative thermodynamic complex (60 min) formed between CRABPII-R111K:R132L:Y134F:T54V:R59W and all-*trans*-retinal (left panel); the PSB pK_a calculated for the thermodynamic product is 2.5 (middle panel); crystal structure of the CRABPII-R111K:R132L:Y134F:T54V:R59W mutant (PDB: 4I9S) with a *trans*-imine conformation (right panel).

On the other hand, the putative *cis* iminium of the retinal-bound R111K:R132L:Y134F:T54V:R59W mutant would orient the proton in a position that would allow for π-cation stabilization via Trp109 (Figure 4a, right).[26] In fact, this interaction has been cited previously as a dominant factor in stabilizing the *cis* iminium with hCRBPII mutants.[9] In such a scenario, the presumed kinetic product, the *cis* iminium, interacting with Trp109, would lose the cationic stabilization upon isomerization to the thermodynamically more stable *trans* imine. The slow isomerization results in a steady decrease in the PSB over time, as observed in Figure 3. Interestingly, looking back at the comparison of entries 3 and 13 in Table 2, with the crystal structure in mind, the effect of the E73A mutation can be rationalized more clearly. As depicted in Figure 4, Glu73 hydrogen bonds to Trp109, orienting it for proper π-cation interaction with the proton of the presumed *cis* iminium (entry 3, pK_a 7.0). Removal of the latter interaction via the E73A mutation leads to a low pK_a complex (2.4), which is likely the result of Trp109 adopting a nonproductive orientation for π-cation interaction. Thus, the *trans* isomer, surrounded by hydrophobic amino acids, predominates by depressing the pK_a of the iminium.[27]

On the basis of the latter rationale, we suggest that the high pK_a variants in Table 2 represent the kinetic isomers that are capable of stabilizing the protonated iminium by the protein surroundings (Figure 4a). Conversely, the low pK_a mutants putatively adopt the structure of the thermodynamic isomer that places the imine in an environment that is devoid of cation-stabilizing elements (Figure 4b). Interestingly, with the exception of the R111K:R132L:Y134F:T54V:R59W CRABPII pentamutant discussed above, which exhibits a *trans* iminium, crystal structures for other mutants (**M1**, **M2**, and **M3**, Table 2) can be refined to accommodate both the *cis* and *trans* iminium geometry (Figure 5). This points to the possibility that both isomeric species can be present and the fact that interconversions between the two states are energetically feasible.

Although it is not possible to extend this analysis with absolute certainty to all the mutants in Table 2, we suggest that

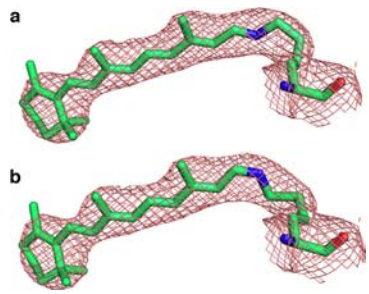

Figure 5. Crystal structure of the CRABPII-R111K:R132L:Y134F:T54V:R59W:A32W bound to all-*trans*-retinal. The electron density around the iminium is broad enough to fit either the *trans* (a) or the *cis* (b) form of the iminium.

dx.doi.org/10.1021/ja404900k | *J. Am. Chem. Soc.* 2013, 135, 16111−16119

protein complexes at the higher pK_a range adopt a *cis* iminium geometry, and conversely the systems exhibiting extremely low pK_a have a *trans* iminium geometry. For mutants with a pathway for isomerization, we observe a time-dependent change in the iminium pK_a. Alterations that lead to changes in overall polarity within each isomeric regime could also further affect the pK_a, a combination of which provides a rich series of mutant proteins that exhibit a range of pK_a values, extending from 8.1 to 2.4. On the other hand, electrostatic perturbations along the polyene that govern the overall absorption of the bound chromophore (as discussed earlier) provide a series of proteins that are variant not only in the pK_a of the PSB but also in their absorption maximum (482−607 nm, Table 2). This unique combination lends itself to the potential use of these protein complexes as chromophoric pH sensors.

Figure 6 visually illustrates the pH dependence of a handful of mutants described in Table 2 in their SB and PSB states. As

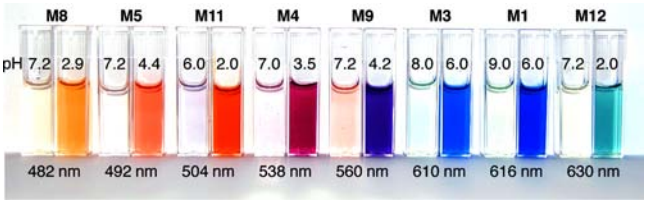

Figure 6. Colorimetric pH response of the various CRABPII mutants: all solutions are pale yellow at basic pH but produce various colors at acidic pH based on pK_a and wavelength of the mutant.

mentioned earlier, the SB for each mutant will absorb in the same region (~365 nm) due to the absence of a resonating positive charge. The protonated states (PSBs), however, absorb at various wavelengths, depending on the effective distribution of the cationic charge along the length of the polyene. What is clearly demonstrated in Figure 6 is the 'on' color state of each mutant at the appropriate pH, dictated by the pK_a of the particular mutant. It is clear that a number of choices are possible, depending on the desired wavelength regime and also the pK_a of the protein.

From the list of proteins in Table 2, the R111K:R132Q:Y134F:T54V:R59W:A32W:M93L:E73A CRABPII mutant (**M12**) bears special mention as a representative, low pH stable protein (the other proteins behaved similarly, however this mutant is discussed in detail since it will be utilized later as a pH sensor). Exhibiting an apparent pK_a of 2.6 (Table 2, entry 9), titration to pH 1.6 proceeds without denaturation of the protein (Figure S8, SI). The protein/retinal complex is highly colored (green) at pH 2 (Figure 6), indicating that the protein is properly folded (denatured protein with the chromophore bound as a retinylidene absorbs at ~440 nm, corresponding to the typical wavelength of absorption for the PSB of retinal).[11] Also, the circular dichroic spectra show little change during acid titration (Figure S8, SI), further suggesting that the protein retains its native fold at low pH. Significant changes in the CD spectra only become apparent at pH of 0.6, concomitant with protein precipitation. The extreme acid stability is most likely due to enhanced hydrophobic packing in the binding cavity. The stability of acid-resistant proteins, typically found in acidophilic organisms, is usually ascribed to increased hydrogen bonding networks and salt bridge interactions,[28] which is in clear contrast to the case reported here.

Ratiometric pH Response of CRABPII Mutants. Genetically encoded pH sensors are of extreme interest for a number of biological applications. Practical pH sensors for use in complex biological systems are fluorescent since absorptive

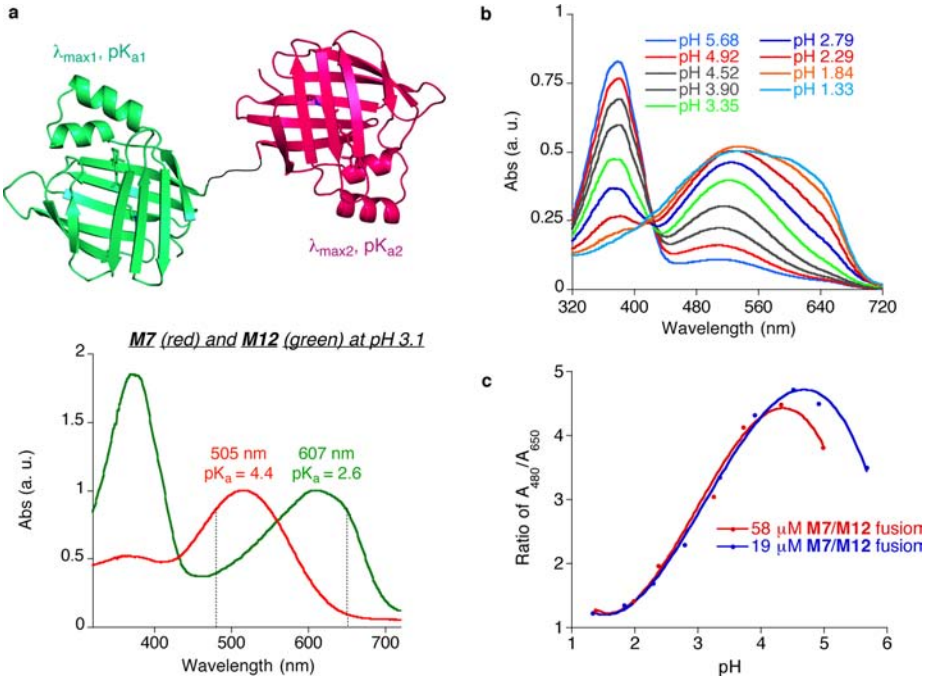

Figure 7. Two-protein-based ratiometric probe design. (a) Selected proteins have distinct wavelength and pK_a values. The UV−vis spectra for **M7** and **M12** at pH 3.1 illustrate the characteristics of each pigment at an intermediate pH relative to their pK_a values. (b) pH titration of the **M7**/**M12** fused protein. (c) Ratiometric analysis of the **M7**/**M12** fused protein system at two different concentrations illustrates the concentration-independent nature of the pH reporter, with reproducible results that span the pK_a of both proteins.

dx.doi.org/10.1021/ja404900k | J. Am. Chem. Soc. 2013, 135, 16111−16119

chromophores most often cannot overcome issues with low sensitivity at low concentrations and also interferences with the biological milieu. Nonetheless, demonstration of pH sensitivity with the chromophoric protein systems described here can be extended to fluorophoric chromophores that have an exchangeable iminium proton. This work is undergoing. Below we present data that describe the development of CRABPII mutants as pH sensors.

To demonstrate a proof-of-principle ratiometric pH sensor with CRABPII mutants, we required the fusion of two colorimetric proteins that had both unique absorptions upon protonation of the Schiff base and distinct pK_a values, such that the extent of protonation for each at the same pH would be different. A fusion construct of the two colorimetric proteins would ensure equal expression of each (Figure 7a). The two reporter proteins would be chosen based on the approximate pH of the system under investigation. The pK_a of the two proteins must be close enough such that in the pH region of interest both proteins respond colorimetrically to the pH change. In this manner, the ratio of two absorptions at specific wavelengths can be correlated to a standard curve.

The criteria for choosing the two proteins for the pH pair were: (1) pK_a ~2 units apart; (2) λ_{max} of absorption >100 nm apart; and (3) similar affinity for retinal. The chosen pair (KLFV:L121Q:R59W (**M7**); pK_a 4.4, λ_{max} 505 nm, K_d 18 nM, and KQFV:R59W:A32W:M93L:E73A (**M12**); pK_a 2.6, λ_{max} 607 nm, K_d 35 nM) meet all the specifications. The first test of the concept was performed with purified proteins that were mixed together at equal ratios (both mutants, at five different concentrations, from 10 to 40 μM, were independently preincubated with 2 equiv of retinal). The protein pair in pH 5.0 citrate buffer was titrated with a strong acid, and UV−vis spectra were recorded (Figure S2a−e, SI). The ratiometric standard curve was generated by plotting the 480/650 nm absorption ratio as a function of the pH, yielding the plot depicted in Figure S2f (SI). The overlap of the data collected at five different concentrations clearly illustrates the concentration-independent nature of the method.

The success in generating a ratiometric standard curve described above prompted the cloning of a fusion pair of the same proteins (**M7** and **M12**), as depicted in the modeled structure in Figure 7a. **M12** (on the N-terminus) and **M7**, separated by a 3-amino acid linker, were cloned and overexpressed in *E. coli*. The isolated protein was incubated with 2 equiv of retinal at room temperature in pH 5 citrate buffer, yielding the spectrum in Figure 7b. Acid titration of the fusion protein complexed with retinal from pH ~5 to ~1, at two dilutions (58 and 19 μM), exhibited the anticipated change in the absorption as dictated by the pK_a of both iminiums bound to each half of the fusion protein. Initially, the absorption with highest intensity was at 510 nm (due to maximum absorption of **M7**) but gradually shifted to longer wavelengths as a result of **M12** absorption (Figure 7b). As depicted in Figure 7c, the final ratiometric scatter plots at two concentrations have practically overlapping ratios between pH of 2 and 4, the working pH range for the chosen protein pairs. The standard curve was utilized to measure the pH of known buffer solutions to within ±0.2 pH units (3.3 measured with a pH meter compared to 3.5 expected from the ratiometric probe). It is important to note that 1 pH unit above the pK_a of the more basic iminium (or 1 pH unit below the pK_a of the more acidic iminium) does not produce reliable results since the absorption of one pigment will not change during the titration. The working range of the probe is identified from the ratiometric scatter plots (in this example, the working pH range is between 2 and 4: **M12** with pK_a 2.6 responds to pH changes between 2 and 4, **M7** with pK_a 4.4 responds to pH changes between 3.4 and 5.4). The importance of a fused construct is clear by comparison of Figure S8 (SI) and Figure 7c where the ratio values for the fusion are different from the ratio obtained from the experiment with two proteins expressed individually. The latter system illustrates a proof-of-principle example of a ratiometric pH sensor that functions with the same chromophore, yet the chromophore not only absorbs at different wavelengths but also changes color at different pH values. Extension of this methodology into a system capable of in vivo applications with fluorescent chromophores is currently underway.

CONCLUSION

In summary the binding pocket of CRABPII, a small cytosolic retinoic acid chaperone protein, has been redesigned to bind retinal as a PSB more deeply in the binding pocket relative to the natural retinoic acid substrate. This system was then used to demonstrate wavelength tuning of the retinal PSB chromophore over a 166 nm range, from 474 to 640 nm, by mutation of only seven positions of the protein. This illustrated the key concepts of wavelength tuning, namely, electrostatic manipulation around the PSB, complete encapsulation of the chromophore, and a uniform electrostatic potential along the polyene by altering the internal electrostatic potential with mutations that lead to only subtle changes in electrostatics, demonstrating that the same principles of wavelength tuning can be applied in disparate protein systems. These colorimetric proteins were then modified to give retinylidene pK_a values from 2.4 to 8.1. Finally a colorimetric pH sensor was constructed using these proteins that measure pH ratiometrically, independent of the concentration of the protein.

ASSOCIATED CONTENT

Supporting Information

Experimental details, protein characterization data, protein crystallographic data, and supplementary figures and tables. The crystal structure of CRABPII-R132K:R111L:L121E was published earlier with accession code 2G7B. The crystal structures of CRABPII-R111K:R132L:Y134F:T54V:R59W, CRABPII-R111K:R132Q:Y134F:T54V:R59W:A32W (**M1**), CRABPII-R111K:R132Y:Y134F:T54V:R59W:A32W (**M2**), and CRABPII-R111K:R132L:Y134F:T54V:R59W:A32W (**M3**) were obtained as a part of this study and deposited to the Protein Data Bank with accession codes 4I9S, 4M7M, 4M6S, and 4I9R, respectively. This material is available free of charge via the Internet at http://pubs.acs.org.

AUTHOR INFORMATION

Corresponding Author

babak@chemistry.msu.edu; geiger@chemistry.msu.edu

Notes

The authors declare no competing financial interest.

ACKNOWLEDGMENTS

The authors thank Professor Daniel Jones (Michigan State University) for help with ESI-TOF of reductively aminated proteins. Generous support was provided by the NIH (GM101353). We are grateful to beam line staff at IMCA-

CAT 32-ID and SBC-CAT 19-ID (supported by the DOE Office of Energy Research, under Contract No. W-31-109-ENG-38). The APS is supported by the U.S. DOE, Office of Science, Office of Basic Energy Sciences, under Contract No. W-31-109-ENG-38.

REFERENCES

(1) (a) Baker, D. *Protein Sci.* **2010**, *19*, 1817. (b) Baker, M. *Nat. Methods* **2011**, *8*, 623. (c) Eiben, C. B.; Siegel, J. B.; Bale, J. B.; Cooper, S.; Khatib, F.; Shen, B. W.; Players, F.; Stoddard, B. L.; Popovic, Z.; Baker, D. *Nat. Biotechnol.* **2012**, *30*, 190. (d) Gordon, S. R.; Stanley, E. J.; Wolf, S.; Toland, A.; Wu, S. J.; Hadidi, D.; Mills, J. H.; Baker, D.; Pultz, I. S.; Siegel, J. B. *J. Am. Chem. Soc.* **2012**, *134*, 20513.

(2) (a) Chen, Z.; Jing, C.; Gallagher, S. S.; Sheetz, M. P.; Cornish, V. W. *J. Am. Chem. Soc.* **2012**, *134*, 13692. (b) Jing, C.; Cornish, V. W. *Acc. Chem. Res.* **2011**, *44*, 784. (c) Los, G. V.; Encell, L. P.; McDougall, M. G.; Hartzell, D. D.; Karassina, N.; Zimprich, C.; Wood, M. G.; Learish, R.; Ohane, R. F.; Urh, M.; Simpson, D.; Mendez, J.; Zimmerman, K.; Otto, P.; Vidugiris, G.; Zhu, J.; Darzins, A.; Klaubert, D. H.; Bulleit, R. F.; Wood, K. V. *ACS Chem. Biol.* **2008**, *3*, 373. (d) Uttamapinant, C.; White, K. A.; Baruah, H.; Thompson, S.; Fernandez-Suarez, M.; Puthenveetil, S.; Ting, A. Y. *Proc. Natl. Acad. Sci. U.S.A.* **2010**, *107*, 10914. (e) Yang, M.; Song, Y.; Zhang, M.; Lin, S.; Hao, Z.; Liang, Y.; Zhang, D.; Chen, P. R. *Angew. Chem., Int. Ed.* **2012**, *51*, 7674.

(3) (a) Wang, Q.; Priestman, M. A.; Lawrence, D. S. *Angew. Chem., Int. Ed.* **2013**, *52*, 2323. (b) Zrazhevskiy, P.; Gao, X. *Nat. Commun.* **2013**, *4*, 1619.

(4) Han, J.; Burgess, K. *Chem. Rev.* **2010**, *110*, 2709.

(5) Subach, F. V.; Verkhusha, V. V. *Chem. Rev.* **2012**, *112*, 4308.

(6) (a) Fu, H.-Y.; Lin, Y.-C.; Chang, Y.-N.; Tseng, H.; Huang, C.-C.; Liu, K.-C.; Huang, C.-S.; Su, C.-W.; Weng, R. R.; Lee, Y.-Y.; Ng, W. V.; Yang, C.-S. *J. Bacteriol.* **2010**, *192*, 5866. (b) Kochendoerfer, G. G.; Lin, S. W.; Sakmar, T. P.; Mathies, R. A. *Trends Biochem. Sci.* **1999**, *24*, 300.

(7) (a) Crist, R. M.; Vasileiou, C.; Rabago-Smith, M.; Geiger, J. H.; Borhan, B. *J. Am. Chem. Soc.* **2006**, *128*, 4522. (b) Vasileiou, C.; Vaezeslami, S.; Crist, R. M.; Rabago-Smith, M.; Geiger, J. H.; Borhan, B. *J. Am. Chem. Soc.* **2007**, *129*, 6140.

(8) Lee, K. S. S.; Berbasova, T.; Vasileiou, C.; Jia, X.; Wang, W.; Choi, Y.; Nossoni, F.; Geiger, J. H.; Borhan, B. *ChemPlusChem* **2012**, *77*, 273.

(9) Wang, W.; Nossoni, Z.; Berbasova, T.; Watson, C. T.; Yapici, I.; Lee, K. S. S.; Vasileiou, C.; Geiger, J. H.; Borhan, B. *Science* **2012**, *338*, 1340.

(10) (a) Kusnetzow, A.; Dukkipati, A.; Babu, K. R.; Singh, D.; Vought, B. W.; Knox, B. W.; Birge, R. R. *Biochemistry* **2001**, *40*, 7832. (b) Spudich, J. L.; Yang, C. S.; Jung, K. H.; Spudich, E. N. *Annu. Rev. Cell Dev. Biol.* **2000**, *16*, 365.

(11) Blatz, P. E.; Tompkins, J. A. *Photochem. Photobiol.* **1993**, *58*, 400.

(12) (a) Feuster, E. K.; Glass, T. E. *J. Am. Chem. Soc.* **2003**, *125*, 16174. (b) Gutierrez-Moreno, N. J.; Medrano, F.; Yatsimirsky, A. K. *Org. Biomol. Chem.* **2012**, *10*, 6960.

(13) (a) Dennis, A. M.; Rhee, W. J.; Sotto, D.; Dublin, S. N.; Bao, G. *ACS Nano* **2012**, *6*, 2917. (b) Schreml, S.; Meier, R. J.; Wolfbeis, O. S.; Landthaler, M.; Szeimies, R.-M.; Babilas, P. *Proc. Natl. Acad. Sci. U.S.A.* **2011**, *108*, 2432. (c) Somers, R. C.; Lanning, R. M.; Snee, P. T.; Greytak, A. B.; Jain, R. K.; Bawendi, M. G.; Nocera, D. G. *Chem. Sci.* **2012**, *3*, 2980. (d) Zhao, L.; Nakayama, T.; Tomimoto, H.; Shingaya, Y.; Huang, Q. *Nanotechnology* **2009**, *20*, 325501.

(14) (a) Bizzarri, R.; Serresi, M.; Luin, S.; Beltram, F. *Anal. Bioanal. Chem.* **2009**, *393*, 1107. (b) Choi, W.-G.; Swanson, S. J.; Gilroy, S. *Plant J.* **2012**, *70*, 118. (c) Llopis, J.; McCaffery, J. M.; Miyawaki, A.; Farquhar, M. G.; Tsien, R. Y. *Proc. Natl. Acad. Sci. U.S.A.* **1998**, *95*, 6803. (d) McAnaney, T. B.; Park, E. S.; Hanson, G. T.; Remington, S. J.; Boxer, S. G. *Biochemistry* **2002**, *41*, 15489. (e) Miesenbock, G.; De Angelis, D. A.; Rothman, J. E. *Nature* **1998**, *394*, 192. (f) Li, Y.; Tsien, R. W. *Nat. Neurosci.* **2012**, *15*, 1047.

(15) (a) Bagar, T.; Altenbach, K.; Read, N. D.; Bencina, M. *Eukaryotic Cell* **2009**, *8*, 703. (b) Disbrow, G. L.; Hanover, J. A.; Schlegel, R. *J. Virol.* **2005**, *79*, 5839. (c) Jankowski, A.; Kim, J. H.; Collins, R. F.; Daneman, R.; Walton, P.; Grinstein, S. *J. Biol. Chem.* **2001**, *276*, 48748. (d) Orij, R.; Postmus, J.; Ter Beek, A.; Brul, S.; Smits, G. J. *Microbiology* **2009**, *155*, 268.

(16) Tantama, M.; Hung, Y. P.; Yellen, G. *J. Am. Chem. Soc.* **2011**, *133*, 10034.

(17) Gjetting, K. S. K.; Ytting, C. K.; Schulz, A.; Fuglsang, A. T. *J. Exp. Bot.* **2012**, *63*, 3207.

(18) (a) Ashby, M. C.; Ibaraki, K.; Henley, J. M. *Trends Neurosci.* **2004**, *27*, 257. (b) Diril, M. K.; Wienisch, M.; Jung, N.; Klingauf, J.; Haucke, V. *Dev. Cell* **2006**, *10*, 233. (c) Granseth, B.; Odermatt, B.; Royle, S. J.; Lagnado, L. *Neuron* **2006**, *51*, 773. (d) Miesenbock, G. *Cold Spring Harbor Protoc.* **2012**, *2012*, 213. (e) Voglmaier, S. M.; Kam, K.; Yang, H.; Fortin, D. L.; Hua, Z.; Nicoll, R. A.; Edwards, R. H. *Neuron* **2006**, *51*, 71.

(19) Wu, M. M.; Llopis, J.; Adams, S. R.; McCaffery, J. M.; Teter, K.; Kulomaa, M. S.; Machen, T. E.; Moore, H. P. H.; Tsien, R. Y. *Appl. Chimeric Genes Hybrid Proteins Part B* **2000**, *327*, 546.

(20) (a) Kralj, J. M.; Douglass, A. D.; Hochbaum, D. R.; Maclaurin, D.; Cohen, A. E. *Nat. Methods* **2012**, *9*, 90. (b) Maclaurin, D.; Venkatachalam, V.; Lee, H.; Cohen, A. E. *Proc. Natl. Acad. Sci. U.S.A.* **2013**, *110*, 5939. (c) Bayraktar, H.; Fields, A. P.; Kralj, J. M.; Spudich, J. L.; Rothschild, K. J.; Cohen, A. E. *Photochem. Photobiol.* **2012**, *88*, 90.

(21) Vasileiou, C.; Lee, K. S. S.; Crist, R. M.; Vaezeslami, S.; Goins, S. A.; Geiger, J. H.; Borhan, B. *Proteins* **2009**, *76*, 281.

(22) It should be noted that though the basic strategy employed to regulate wavelength in the CRABPII system is similar to that used for hCRBPII and although two wild-type proteins share almost identical tertiary structure, they have only 38% sequence identity if aligned in BLAST. All mutations, save those that close the binding pocket (by mutation of the R59 (R58 in CRBPII) and the A32 positions (A33 in CRBPII)), are different in CRABPII due to the distinctly different electrostatic environments of the two proteins.

(23) (a) Sakmar, T. P.; Franke, R. R.; Khorana, H. G. *Proc. Natl. Acad. Sci. U.S.A.* **1991**, *88*, 3079. (b) Sheves, M.; Albeck, A.; Friedman, N.; Ottolenghi, M. *Proc. Natl. Acad. Sci. U.S.A.* **1986**, *83*, 3262. (c) Steinberg, G.; Ottolenghi, M.; Sheves, M. *Biophys. J.* **1993**, *64*, 1499. (d) Zhukovsky, E. A.; Oprian, D. D. *Science* **1989**, *246*, 928.

(24) (a) Baasov, T.; Sheves, M. *Biochemistry* **1986**, *25*, 5249. (b) Rousso, I.; Friedman, N.; Sheves, M.; Ottolenghi, M. *Biochemistry* **1995**, *34*, 12059.

(25) (a) Luecke, H.; Schobert, B.; Richter, H. T.; Cartailler, J. P.; Lanyi, J. K. *J. Mol. Biol.* **1999**, *291*, 899. (b) Murakami, M.; Kouyama, T. *Nature* **2008**, *453*, 363. (c) Shibata, M.; Tanimoto, T.; Kandori, H. *J. Am. Chem. Soc.* **2003**, *125*, 13312. (d) Sekharan, S.; Wei, J. N.; Batista, V. S. *J. Am. Chem. Soc.* **2012**, *134*, 19536.

(26) The *cis* iminium model depicted in Figure 4a was generated from the crystal structure of the *trans* iminium observed in the crystal structure of R111K:R132L:Y134F:T54V:R59W, details of which are described in the SI.

(27) Mutations of Trp109 were attempted to examine its effect on the stability of the PSB. However, replacement of Trp109 with a variety of amino acids did not yield proteins that could be expressed solubly.

(28) (a) Fushinobu, S.; Ito, K.; Konno, M.; Wakagi, T.; Matsuzawa, H. *Protein Eng.* **1998**, *11*, 1121. (b) Nonaka, Y.; Akieda, D.; Aizawa, T.; Watanabe, N.; Kamiya, M.; Kumaki, Y.; Mizuguchi, M.; Kikukawa, T.; Demura, M.; Kawano, K. *FEBS J.* **2009**, *276*, 2192. (c) Schwermann, B.; Pfau, K.; Liliensiek, B.; Schleyer, M.; Fischer, T.; Bakker, E. P. *Eur. J. Biochem.* **1994**, *226*, 981. (d) Vinther, J. M.; Kristensen, S. M.; Led, J. J. *J. Am. Chem. Soc.* **2011**, *133*, 271.